

*Mini review*

## Progress in the Photoelectrochemical Biosensors for the Detection of MicroRNAs: A Review

*Linlin Hou<sup>1\*</sup>, Binbin Zhou<sup>1,3</sup>, Yuxin Li<sup>1</sup> and Ming La<sup>2\*</sup>*

<sup>1</sup> Henan Province of Key Laboratory of New Optoelectronic Functional Materials, College of Chemistry and Chemical Engineering, Anyang Normal University, Anyang, Henan 455000, People's Republic of China

<sup>2</sup> College of Chemistry and Chemical Engineering, Pingdingshan University, Pingdingshan, Henan 467000, People's Republic of China

<sup>3</sup> Hunan Institute of Food Quality Supervision Inspection and Research, Building B, No. 238, Ave. Timesun, District Yuhua, Changsha, Hunan 410111, People's Republic of China

\*E-mail: [linlin9918@163.com](mailto:linlin9918@163.com) (L. H.); [mingla2011@163.com](mailto:mingla2011@163.com) (M. L.)

Received: 7 January 2019 / Accepted: 13 February 2019 / Published: 10 April 2019

MicroRNAs (miRNAs) have been regarded as the new targets for cancer diagnosis and treatment. Photoelectrochemical (PEC) biosensors with the advantages of miniaturization, high sensitivity and low background signal have been developed for miRNAs detection in recent years. This work focused on the recent progress in the design strategies for miRNAs detection with PEC biosensors.

**Keywords:** MicroRNAs; photoelectrochemistry; biosensors;

### 1. INTRODUCTION

MicroRNAs (miRNAs) are a class of 21 ~ 25mer long non-protein-coding small RNAs found in eukaryotes. They can degrade or inhibit the translation of target gene through complete or incomplete matching with target gene 3'UTR, thus accurately regulating the development, differentiation, proliferation, apoptosis and immune regulation of organisms [1]. Recently, abnormal expression of miRNAs has been found in a variety of tumors, which is closely related to the progress, clinical treatment and prognosis of tumors [2, 3]. Therefore, miRNAs have become the new targets for cancer diagnosis and treatment [4-6].

As a branch of biosensors for nucleic acid analysis, photoelectrochemical (PEC) biosensors have been significantly flourishing in bioanalysis in view of their characteristic: miniaturization, high

sensitivity and low background signal. They have been recently used in bio-immunoassay, medical diagnosis, food and environmental monitoring, and have become one of the important methods for in vitro diagnosis with the discovery of novel PEC materials [7]. Recently, we and other groups have addressed the progress in the electrochemical and optical detection of miRNAs [1, 8-11]. However, to the best of our knowledge, there is no specific review paper focusing on the progress in the design strategies for miRNAs detection with PEC biosensors. In this review, we summarized the design of PEC miRNAs biosensors developed especially in recent three years (2016 - 2018).

## 2. STRATEGIES FOR PEC DETECTION OF MIRNAS

In general, the detection mechanism of the PEC biosensors for nucleic acid analysis is based on the changed electrical signal upon illumination. In brief, photoactive species employed as the transducers can be captured by the chosen probe DNA, which was monitored by the changed electrical signal of the formation process of numerous DNA-related interactions. The substrates of PEC biosensors influence exquisitely their analytical performance. As to the immobilization of recognition layer for targets, the type and quality of the photoactive species are of vital. Usually, the selection of transducer type is mainly related to the hybridization-related interactions of interest and the proposed analysis strategies. Many hybridization-related interactions can be used for specific analytical purposes based on the selected probe DNA layers fixed on specific sensor surfaces. Commonly, the interactions include three main categories: DNA hybridization, DNA association with small molecules, and DNA-protein interaction. The signal can be amplified by the indicators of quantum dots (QDs) and their composites, nanomaterials, enzymes and so on. The progress in the developed strategies with these signal labels has been addressed herein.

### 2.1. *QDs and their composites*

QDs, also known as semiconductor nanocrystals, are a kind of nanomaterials composed of II-IV or III-V elements with a size of 1-100 nm. They have the advantages of wide excitation spectrum, narrow and symmetrical emission spectrum, high quantum yield and good optical stability [12]. QDs and their composites as photoelectric active materials have shown great potential in traditional and emerging fields such as life science, analytical science, material science, immunomedicine, inspection and quarantine [13]. Wang and Yin have designed a new PEC genesensor for the sensitive determination of miRNA-21 with CdSe QDs as signal labels [14]. The TiO<sub>2</sub>NTs/RGO/AuNPs were used as the photoactive materials, and the photocurrent intensity decreased because of the weakened sensitization influence on condition that the miRNA-21 hybridized with the complementary part of the HP-DNA. The biosensor has a detection limit down to 5.6 fM. A wide linear range (20 fM ~ 0.2 nM) was obtained. The method exhibited good specificity, reproducibility and stability. Moreover, Chen's group developed a PEC biosensor for miRNAs detection based on the exciton-plasmon interactions (EPI) between CdS QDs and Ag nanoparticles (Figure 1) [15]. This strategy is based on the transition of the interparticle interplay from the QDs-Au NPs to the QDs-Ag NPs systems. The target miRNAs can trigger the conformational change of probe from hairpin format to "Y" shape in the presence of biotinylated assistant DNA probe. As a result, streptavidin-labeled alkaline phosphatase (ALP) can be captured through the biotin-

streptavidin interaction, which facilitated the generation of AA and triggered the transition of the interparticle interplay from the QDs-Au NPs to the QDs-Ag NPs. The latter exhibited higher quenching efficiency in contrast to the former. Thus, the target miRNAs can induce the signal change. The linear range for miRNAs detection was 1 fM ~ 100 pM. The detection limit was calculated to be 0.2 fM.

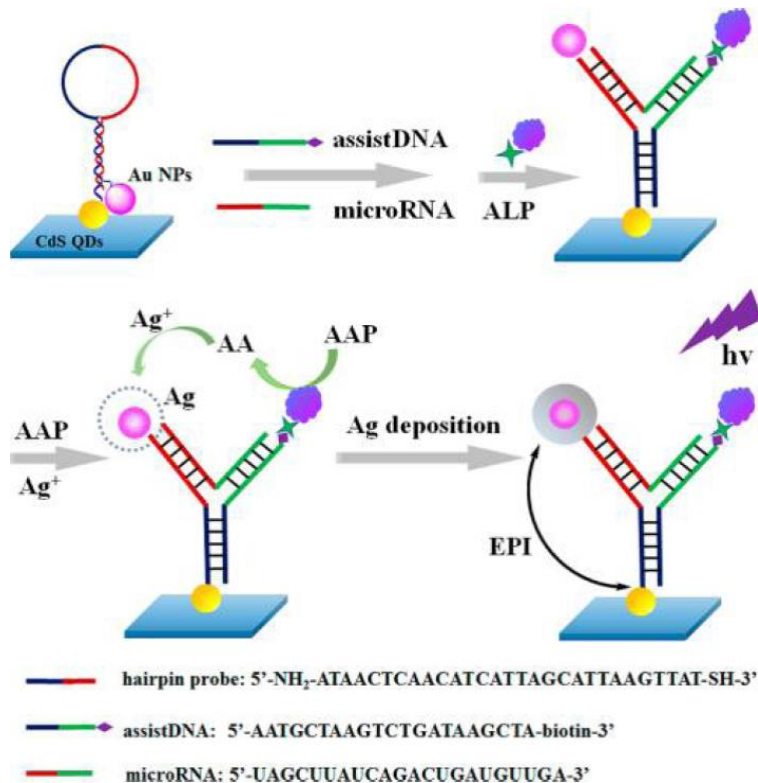


**Figure 1.** Novel PEC microRNA bioassay based on the ingenious transition of the interparticle interplay from the CdS QDs-Au NPs to the CdS QDs-Ag NPs system. Reprinted with permission from reference [15]. Copyright 2018 American Chemical Society.

Another type of QDs-based indicator utilized for sensitive determination of miRNA-141 was DNA tetrahedron (TET)-CdTe QDs-methylene blue (MB) (TET-QDs-MB complex) (Figure 1) [16]. With the complex as an efficient PEC signal indicator, the proposed PEC biosensor performed a wide linear range of 50 aM ~ 50 pM with a low detection limit of 17 aM. The signal was amplified by the duplex specific nuclease (DSN) enzyme-assisted target cycling. Specifically, QDs were bound to the TET through the hybridization. After that, MB molecules as the signal enhancers were inserted to the duplexes on the TET-QDs. The resulting TET-QDs-MB complexes were employed as the efficient signal probes because of their excellent photovoltaic property. The method did not require direct modification of photoactive material on the sensor surface. This improved detection sensitivity by producing a near-zero background noise.

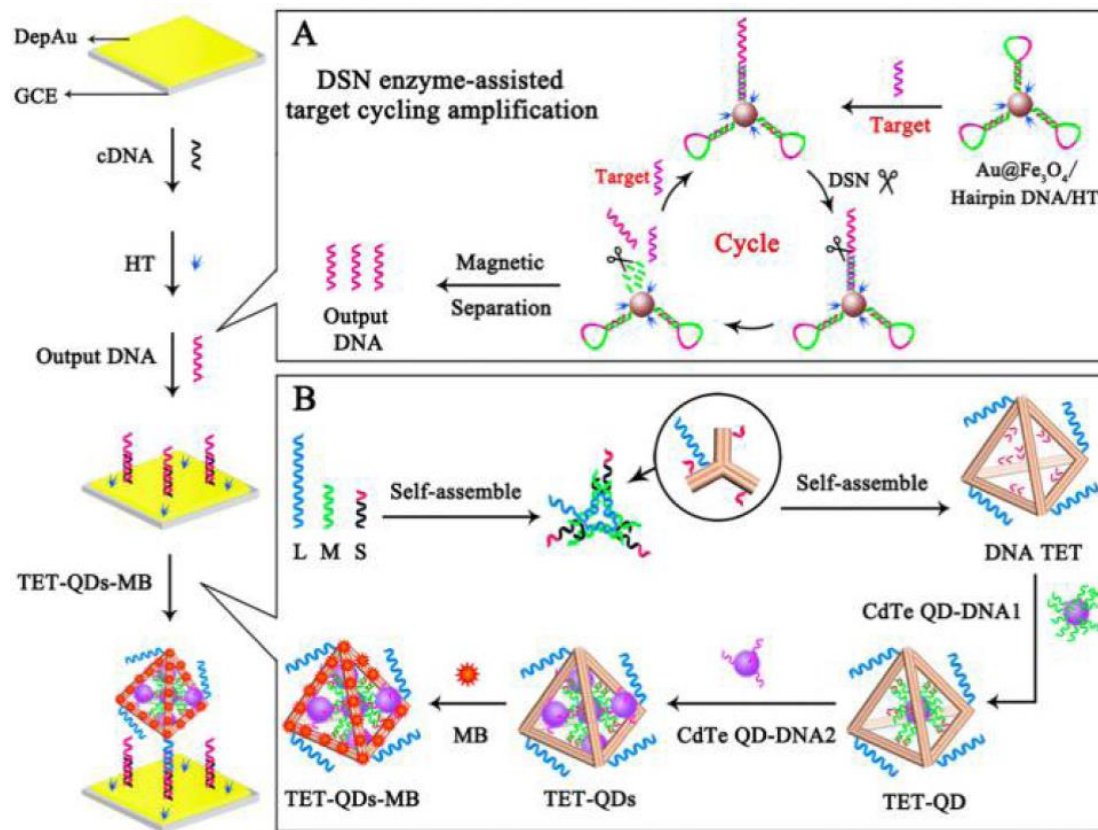


**Figure 2.** Schematic diagrams of this proposed PEC biosensor for miRNA-141 determination; (A) DSN enzyme-assisted target cycling amplification strategy; (B) Preparation of the DNA TET-CdTe QDs-MB complex. Reprinted with permission from reference [16]. Copyright 2016 American Chemical Society.

In addition to the inorganic semiconductors, QDs composites can improve the electron capture and transmission of luminescent semiconductors, including AuNPs/TiO<sub>2</sub>NTs/RGO, TiO<sub>2</sub>-CdS:Mn, CH<sub>3</sub>NH<sub>3</sub>PbI<sub>3</sub>/ZnO and SiO<sub>2</sub>@MB/CdS. An universal ratiometric PEC bioassay was readily achieved for the ultrasensitive detection of miRNA-21 in Yuan's group [17]. The method is based on two different photoactive materials and the photocurrent signals at the wavelength of 460 nm and 623 nm (Figure 3). In the existence of target, the photocurrent signals were changed at the wavelength of 460 nm and 623 nm. Thus, the ratiometric strategy could be realized by monitoring the ratio of the two different PEC signals ( $I_{MB}/I_{QDs}$ ). The method overcomes the high dependence of targets upon photoactive substances.

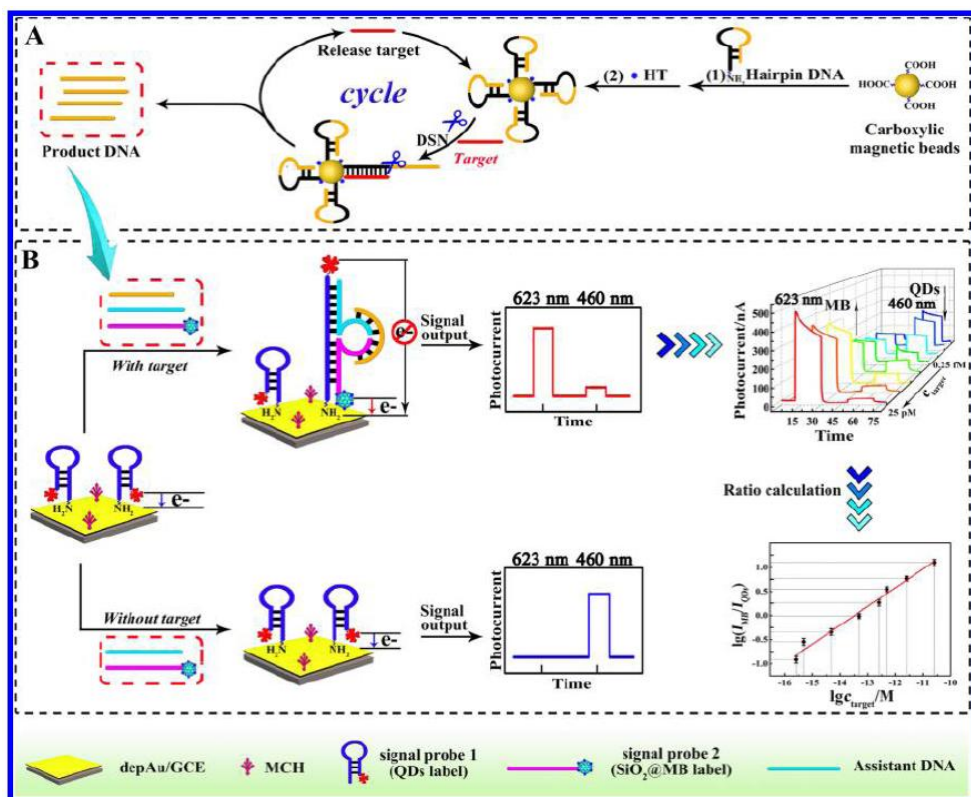


**Figure 3.** Schematic diagram of (A) signal transduction-amplification strategy and (B) Fabrication procedure for the ratiometric PEC assay. Reprinted with permission from reference [17]. Copyright 2017 American Chemical Society.

## 2.2 Enzyme labels

AA, a well-known electron donor, has been widely used in solar energy conversion system. ALP can catalyze the hydrolysis of L-ascorbic acid 2-phosphatase substrate (AAP) to release AA in situ. The resulting AA can reduce  $\text{AuCl}^{4-}$  or  $\text{Ag}^+$  into Au or Ag [18-20]. Recently, the possibility of the possibility of in situ synthesis of AA by enzymatic methods as biosensors has been investigated [21-28]. Remarkably, a photosensitization process took place on the surface of Au NR of nanostructured  $\text{TiO}_2$  electrode after the hybrid triggering enzyme reaction to produce AA, thus allowing for the PEC detection under visible-light illumination. Based on the theory, Bettazzi et al. prepared Au nanorods (NRS)-modified nano-titanium dioxide/ITO electrode for PEC detection of miRNA [21]. DNA capture probes (CPs) were attached onto the Au NR surface. The modified Au NR was chemically anchored on the surface of titanium dioxide/ITO electrode with mercaptosuccinic acid (MSA). Subsequently, the CPs bound to the Au NR surface through thioacid group and react with target miRNA sequence. The biosensor was incubated with ALP and AAP to produce AA. The AA molecules coordinated with Ti atoms on the surface led to the generation of charge transfer complexes, thus leading to the shift of ultraviolet absorption threshold to the visible spectral region of nano-titanium dioxide and producing an absorption band centered at 450 nm. Under visible LED light, the formation of AA-titania complex was monitored by PEC. The target microRNA was selectively and quantitatively determined. In addition, Yang's group developed a new liposome-amplified PEC method for the detection of miRNAs [22]. ALP

was encapsulated in the hydrophilic cavity and streptavidin was modified on the surface of liposome. The ALP-liposome signal label can be captured by the hairpin DNA probe immobilized on the electrode surface in the presence of target miRNAs through the biotin-streptavidin interaction. After addition of Tween-20, the ALP molecules were released to catalyze the hydrolysis of AAP. Moreover, Ai and co-workers also reported the detection of miRNA-319a based on g-C<sub>3</sub>N<sub>4</sub>-AuNPs photoactive substance and in-situ electron donor technology [23]. Graphene-like C<sub>3</sub>N<sub>4</sub> (g-C<sub>3</sub>N<sub>4</sub>) was used as photoactive substance and anti-DNA: RNA antibody was used as the recognition unit for target microRNA. The doping of AuNPs improved the photoactivity of g-C<sub>3</sub>N<sub>4</sub>. MiRNAs were captured by the capture probes assembled on AuNPs-g-C<sub>3</sub>N<sub>4</sub> modified ITO surface. The antibody was recognized and captured by the DNA: RNA hybrids. ALP-labeled IgG (ALP-IgG) was then captured by the specific interaction, which catalyzed the hydrolysis of AAP to AA as an electron donor to trap the holes of g-C<sub>3</sub>N<sub>4</sub>. The method was used to monitor the expression of miRNA-319a in rice leaves. The linear range was 5 ~ 3000 fM and the detection limit was 2.26 fM.

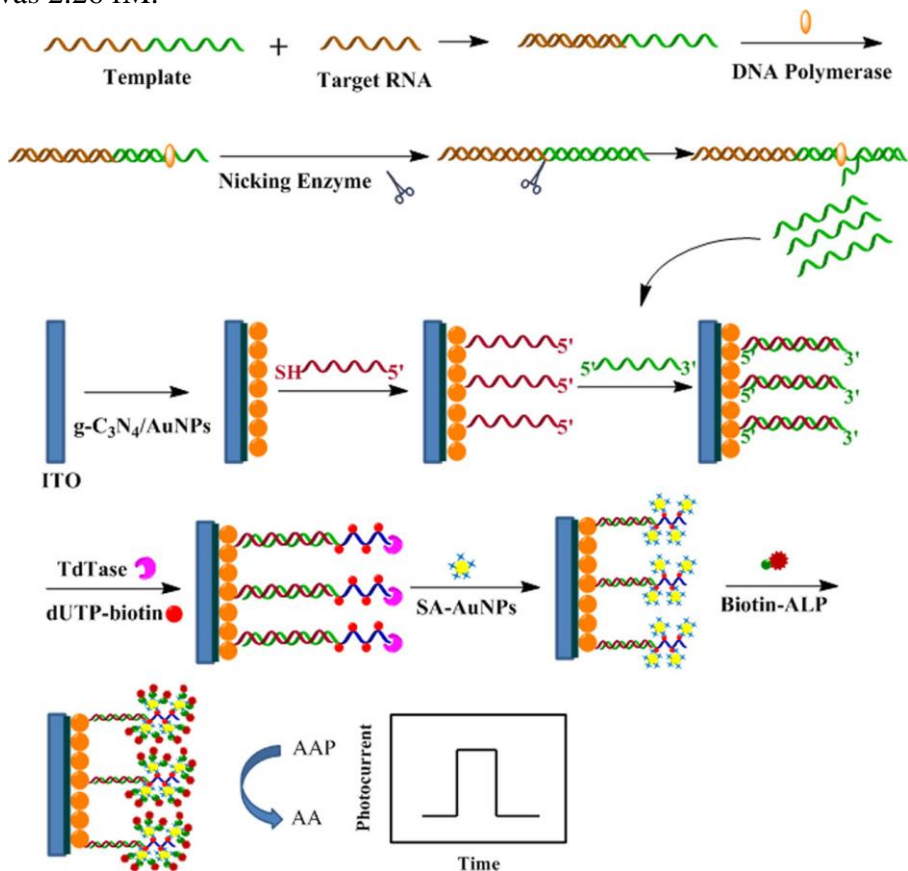


**Figure 4.** Schematic illustration of the PEC biosensor fabrication process. Reprinted with permission from reference [24]. Copyright 2018 Springer Nature.

Furthermore, Ai and co-workers realized the sensitive detection of miRNA-162a in Maize Seedlings with the PEC biosensor based on multiple amplification strategy (Figure 4) [24]. The signal was amplified by isothermal chain displacing polymerase chain reaction (ISDPR), TDT-mediated amplification, streptavidin-coated gold nanoparticles (SA-AuNPs) and biotin-ALP. The ISDPR and TDT-mediated amplification was carried out by generating or extending DNA strands. Catalytic

hydrolysis of AAP to AA electron donor significantly enhanced the photocurrent response. The linear range was 0.5 fM ~ 1 pM and the detection limit was 0.18 fM. For the detection of miRNA-319a, Ai's group also established a simple and sensitive PEC method with CuO-CuWO<sub>4</sub> as photoactive substance [25]. Rolling cycle amplification (RCA), nick endonuclease triggering target molecule exponential amplification, phosphoric acid group and phos-tag catalytic signal amplification technology, biotin-avidin interaction and other advantages greatly improved the detection sensitivity. The linear range was 1 fM ~ 0.1 nM and the detection limit is 0.47 fM.

### 2.3. Metallic nanolabels

For DNA hybridization biosensors, probe DNA with known nucleotide sequences is usually fixed on the surface of the biosensor as a bio-recognition element, and then interacts with target DNA in sample solution. Yu and co-workers constructed a cascade signal amplification platform through DSN-assisted target recycling with catalytic hairpin assembly (CHA) reaction for the detection of miR-141 (Figure 5) [29]. The strategy driven by DSN resulted in significant amplification translation of target miRNA to ssDNA fragments. Meanwhile, the CHA reaction is also triggered by connector DNA with hairpin-modified AuNPs (HP-AuNPs) as the sensor unit. The formation of AuNPs network architecture on electrode surface facilitated the detection of miRNAs down to 25.1 aM. Wang et al. reported a simple PEC biosensor for miRNA-21 detection based on energy transfer (ET) between CdS:Mn doped structure (CdS:Mn) and Au-nanoparticles (AuNPs) [30]. In the presence of miRNA-21, the hairpin DNA was hybridized with miRNA-21, which made AuNPs detached from the electrode surface, resulting in a significant recovery of photocurrent because of the ET effect between CdS:Mn and AuNPs. The sensitive detection of miRNA-21 was realized in a linear range of 1 fM to 10 pM with a low detection limit of 0.5 fM. Moreover, Liu and co-workers reported the high sensitivity and specificity of detection of miRNA-21 based on the EPI between CdS@g-C<sub>3</sub>N<sub>4</sub> heterojunction and Au@Ag nanoparticles (NPs) [31]. The detection principle is shown in Figure 6. The CdS@g-C<sub>3</sub>N<sub>4</sub> nanowires were used as the electrode materials. In the presence of target miRNAs, the hairpin DNA probe immobilized on the electrode surface was opened. The resulting DNA-miRNA duplex can be cleaved by DSN to release miRNA. The released miRNA was then hybridized with another hairpin DNA probe to promote the cyclic reaction and amplify the signal. In the detection step, the DNA-functionalized Au@Ag labels were captured by the sheared capture DNA probes through hybridization. As a result, the EPI between CdS@g-C<sub>3</sub>N<sub>4</sub> nanowires and Au@Ag NPs occurred under light illumination. This resulted in a great decrease in the PEC signal. Based on the EPI sensing mechanism and the DSN-assisted amplification, the PEC biosensor exhibits a linear range of 0.1 ~ 0.1 nM for miRNAs detection.

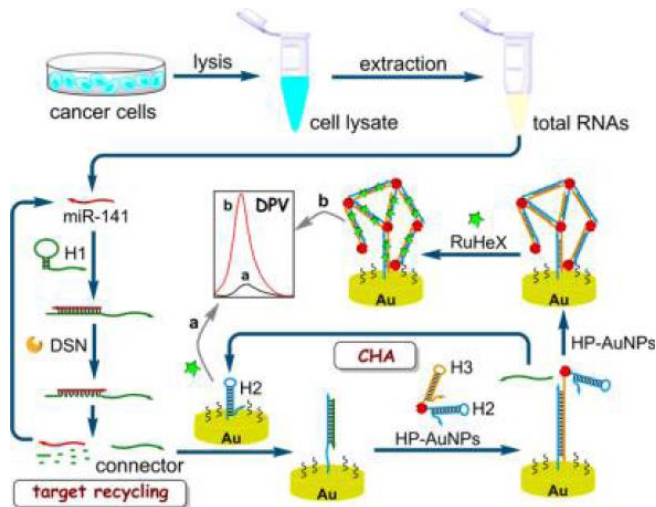


**Figure 5.** Schematic illustration of cascade amplification of DSN-assisted target recycling and CHA reaction. Reprinted with permission from reference [29]. Copyright 2018 American Chemical Society.

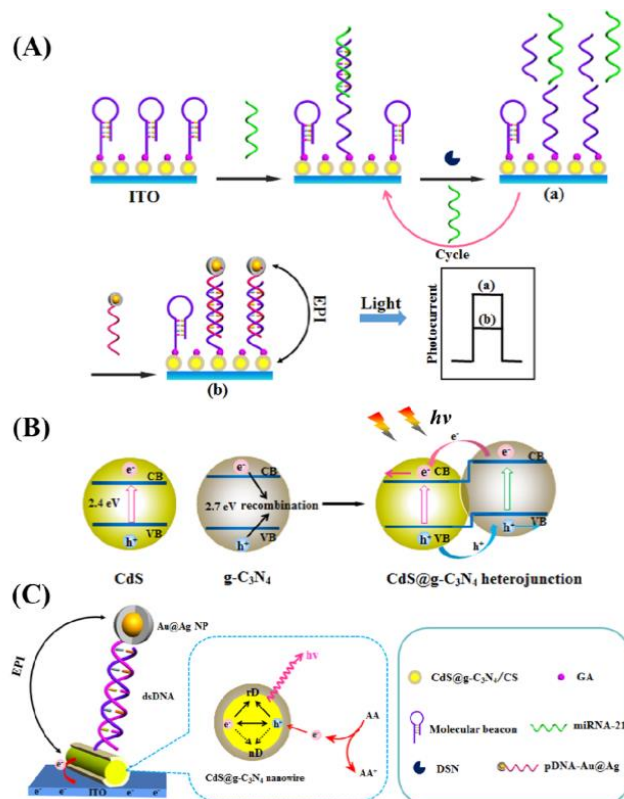


**Figure 6.** (A) Schematic illustration of the fabrication process of the PEC biosensor. (B) Schematic illustration for the energy bands of CdS@ $\text{g-C}_3\text{N}_4$  before and after coupling. (C) Charge transfer process at the formed heterojunction under light illumination. Reprinted with permission from reference [31]. Copyright 2017 American Chemical Society.

$\text{Bi}_2\text{S}_3$  has the advantages of narrow band gap, non-toxicity, low cost, visible light absorption and less environmental pollution [32]. Very recently, with  $\text{Bi}_2\text{S}_3$  nanorods as photoactive materials of PEC biosensors, miRNAs have also been detected with satisfactory results [26, 28]. For example, the  $\text{Bi}_2\text{S}_3$ -based composites with specific architectural morphology by anchoring the 2D layered materials

molybdenum disulfide ( $\text{MoS}_2$ ) to  $\text{Bi}_2\text{S}_3$  possess excellent photocatalytic performance [33]. Wang's group developed a hybridization chain reaction (HCR)-based PEC method for detection of miRNA-141 in prostate cancer cells using dopamine (DA) electron donor assembled together probe- $\text{N}_3$  (denoted as PDA- $\text{N}_3$ ) (Figure 7) [34]. In this method,  $\text{Bi}_2\text{S}_3@\text{MoS}_2$  nanoparticles exhibiting high photoactivity under visible light irradiation made the consumption of DA electron donors. The sensor has a linear detection range of  $0.1 \text{ fM} \sim 0.5 \text{ nM}$  with a detection limit of  $27 \text{ aM}$ .

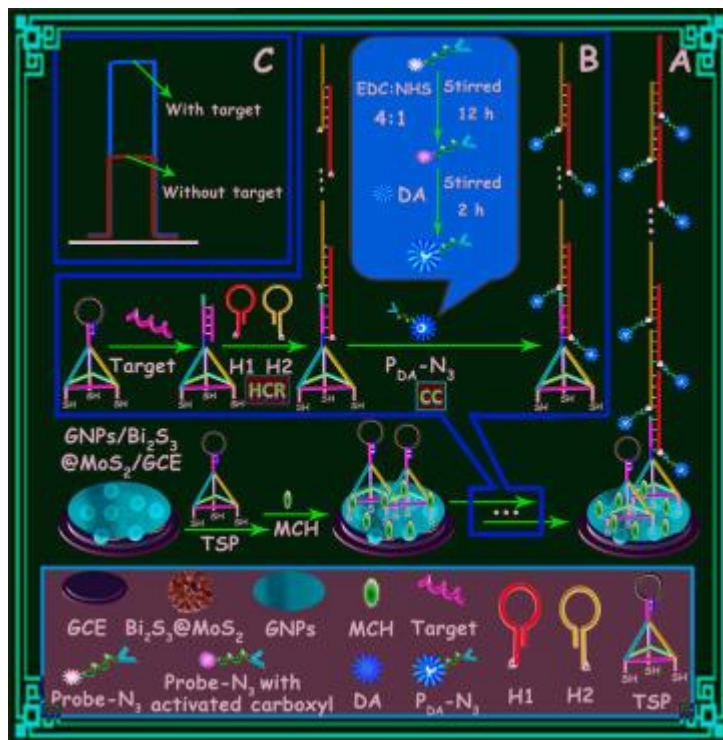


**Figure 7.** Schematic illustration of (A) PEC platform for MiRNA assay; (B) principle of Metal-catalyst-free click chemical signal amplification via hybridization chain reaction (The blue box presents the fabrication process of PDA- $\text{N}_3$ ); and (C) PEC response in the absence and presence of target. Reprinted with permission from reference [34]. Copyright 2016 American Chemical Society.

Metal oxides such as  $\text{PbO}$ ,  $\text{Fe}_2\text{O}_3$ ,  $\text{Co}_3\text{O}_4$ ,  $\text{BiVO}_4$  and  $\text{TiO}_2$  doped with metal can also be used in PEC sensing devices because of their high photocatalytic activity in aqueous phase oxidation. For example, based on hematite orderly ( $\alpha\text{Fe}_2\text{O}_3$ )-coated titanium dioxide nanorods array ( $\text{TiO}_2$  NRAs), Cui and co-workers reported a new approach alternative for the detection of miRNA-21 [35]. In the presence of miRNA-21, this system was triggered to induce a quickly release of the  $\text{Cu}^{2+}$  capped in the mesoporous silica nanomaterial (MSN). As an electron acceptor, the released  $\text{Cu}^{2+}$  was reduced to  $\text{Cu}^{\circ}$  at the reverse electrode, which improved the separation efficiency of electron holes and led to enhanced photocurrent response. This biosensor facilitated the quantitative determination of miRNA-21 in the linear range of  $1 \text{ fM} \sim 150 \text{ pM}$  with a detection limit of  $0.74 \text{ fM}$ . Pang and co-workers developed an ultrasensitive PEC biosensor for the quantitative detection of miRNA-155 with  $\text{ZnO}@\text{CH}_3\text{NH}_3\text{PbI}_3$  as the photoactive material [36]. The significant decrease of the PEC signal could be achieved due to the larger steric hindrance. The linear detection range is  $0.01 \text{ fM} \sim 20 \text{ nM}$ .

## 2.4 Small molecules

For disease diagnosis and drug discovery, it is often important to study the association of DNA with small molecules such as drugs and chemicals. Luo and Li constructed a label-free PEC biosensor based on DNA four-way (4J) and G-wire signal amplification strategy for the determination of miRNA in cancer cells (Figure 8) [37]. The biosensor employed ultrafine copper phosphate nanosheet (CuPi NSs)-coated AuNPs (Au-CuPi NSs) as the photocathode materials to enhance photocurrent response. The quenchers of AuNPs were applied to turn off the PEC signal due to the surface plasmon resonance (SPR) absorption. This allowed for the construction of the unlabeled switch-on PEC platform. MiRNAs were introduced by the DNA four-way junction (4J) structure and quantified through the proportional output of c-myc region. With G-wire structure, 5,10,15,20-tetra(4-sulfophenyl)-21H,23H-porphyrin (TSPP) was coupled on the substrate as the PEC enhancer for the first time. The detection limit for miRNAs in prostate cancer cell 22Rv1 was 4.8 aM.

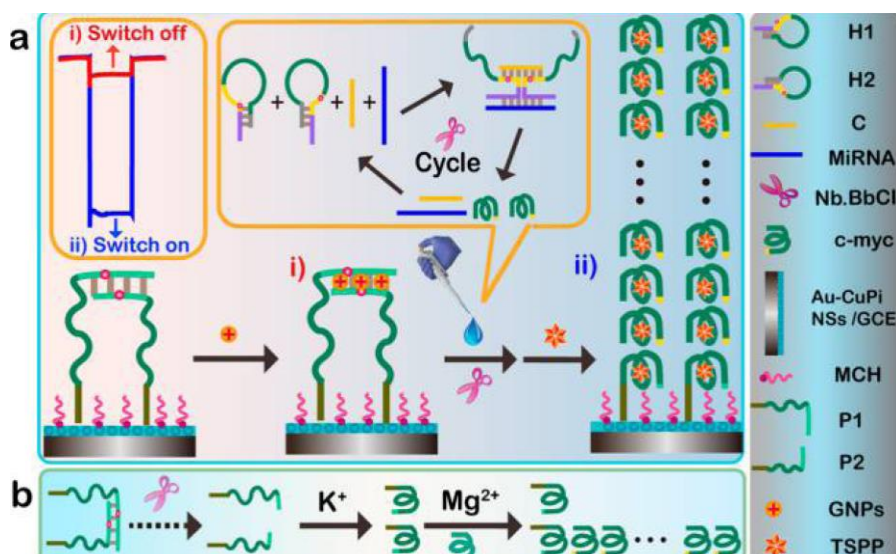


**Figure 8.** Schematic diagrams of (a) the label-free “Off–On” PEC platform fabrication for miRNA assay and (b) the G-wire formation. Reprinted with permission from reference [37]. Copyright 2017 American Chemical Society.

Zheng and Liang reported a self-enhancing PEC biosensor based on the functionalized nano-encapsulated donor-acceptor photoactive substance and its photo sensitizer (Figure 9) [38]. The method had been applied in ultrasensitive detection of miRNA-141 in cancer cells. Multifunctional polymer polyethylene glycol (PEG) with good biocompatibility and film-forming ability as a self-enhancing photoactive material were used to encapsulate the donor-receptor type photoactive material (PTB7-TH) and its photosensitizer fullerene (Nano-C<sub>60</sub>) to form nanocapsule (PCP Nano Capsule). Using the target enzyme-induced double-cycle strategy, hairpin DNA on nano-SiO<sub>2</sub> (NPS) could be cut in the presence of the target and the hybridized with the captured DNA on the modified electrode surface. This induced an increase in electrode steric hindrance and a decrease in initial photocurrent signal. Without any co-reactant or photosensitizer in the test electrolyte, the method realized the quantitative detection of

miRNAs with high accuracy and sensitivity.

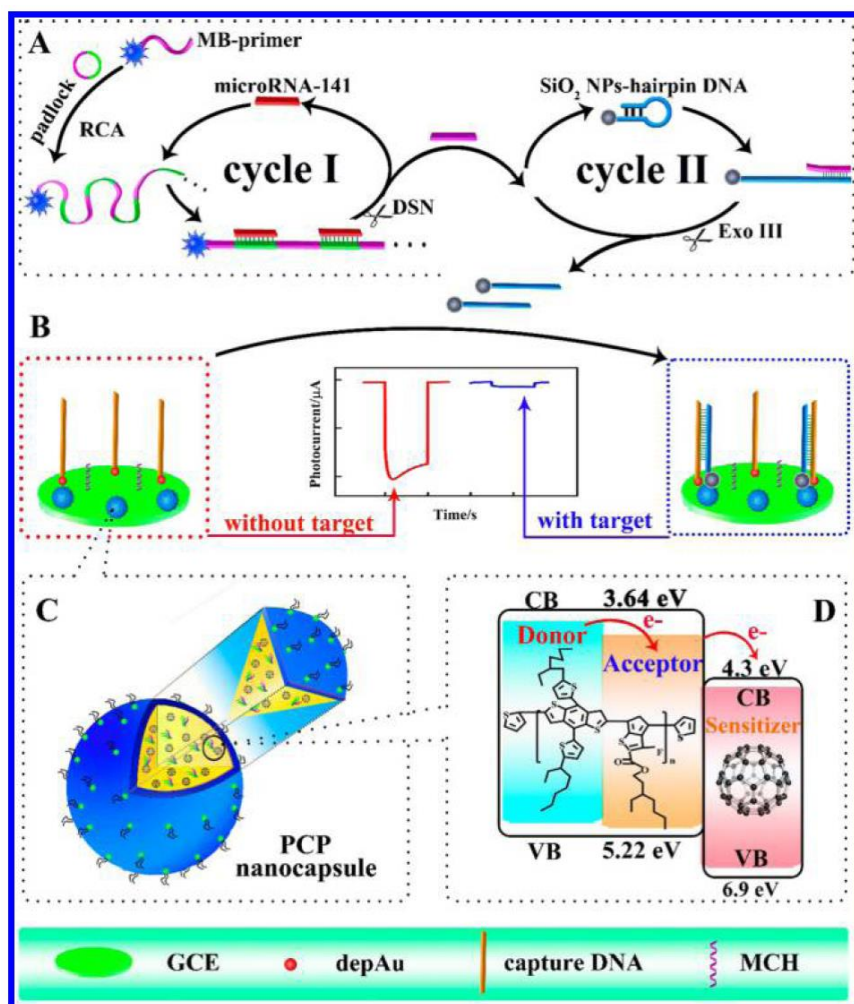


**Figure 9.** Schematic diagram of (A) quadratic enzymes-assisted target recycling amplification strategy for the biosensor, (B) fabrication of the biosensor, (C) enlarged view of PCP nanocapsule, and (D) the electron-transfer route in the PCP nanocapsule. Reprinted with permission from reference [38]. Copyright 2016 American Chemical Society.

## 2.5 Protein interaction

All functions of DNA depend on its interaction with various proteins. Some proteins can bind to DNA nonspecifically or specifically. Enzymes can also bind to DNA to achieve their biological functions. Based on the interaction between DNA and protein, the research of DNA biosensor mainly focuses on two aspects: affinity binding of DNA and protein, enzymatic DNA transformation using DNA-modified enzymes to prepare biometric formats, or direct detection of their catalytic activity. Among many DNA-binding proteins, a unique group binds to a specific DNA sequence. Adsorption of proteins on electrode surface can produce remarkable steric hindrance. For this consideration, several groups have designed novel PEC biosensors for miRNAs detection. Ai's group first reported a PEC

biosensor for miRNAs detection by protein-induced steric hindrance using the  $\text{Bi}_2\text{S}_3$  nanorods as photoactive materials [39]. The binding of streptavidin to biotin DNA produced a significant steric hindrance under the condition of the stem-ring structure of probe DNA hybridized with the target miRNA.  $\text{Bi}_2\text{S}_3$  nanorods synthesized by a hydrothermal method were deposited on the ITO slices for modification with AuNPs. The biotinylated hairpin probes were immobilized on the AuNPs surface through the Au-S interaction. The stem-ring structure of DNA probe was opened after hybridization with target miRNA. Exposure of biotin on the electrode surface allowed for the adsorption of streptavidin through the strong streptavidin-biotin interaction. This produced a steric hindrance to block AA approaching to the electrode surface, thus reducing the photocurrent. The method exhibited a detection limit down to 3.5 fM and can determine single mismatched miRNAs very well. Recently, Zhao and co-workers constructed a sensitive and selective PEC biosensor for the detection of miRNAs in human serum using MoS-AuNPs nanosheets as the electrode materials [40]. AuNPs acted as both the photoelectric transfer promoters and the DNA probe carriers. The hybridization of miRNAs with the DNA capture probe opened the hairpin structure, facilitating the attachment of streptavidin on the electrode surface. The formation of biotin-streptavidin complexes decreased the photocurrent change because of the steric hindrance. The linear range of this method for miRNA detection is 10 fM ~ 1 nM. The detection limit is down to 4.21 fM.

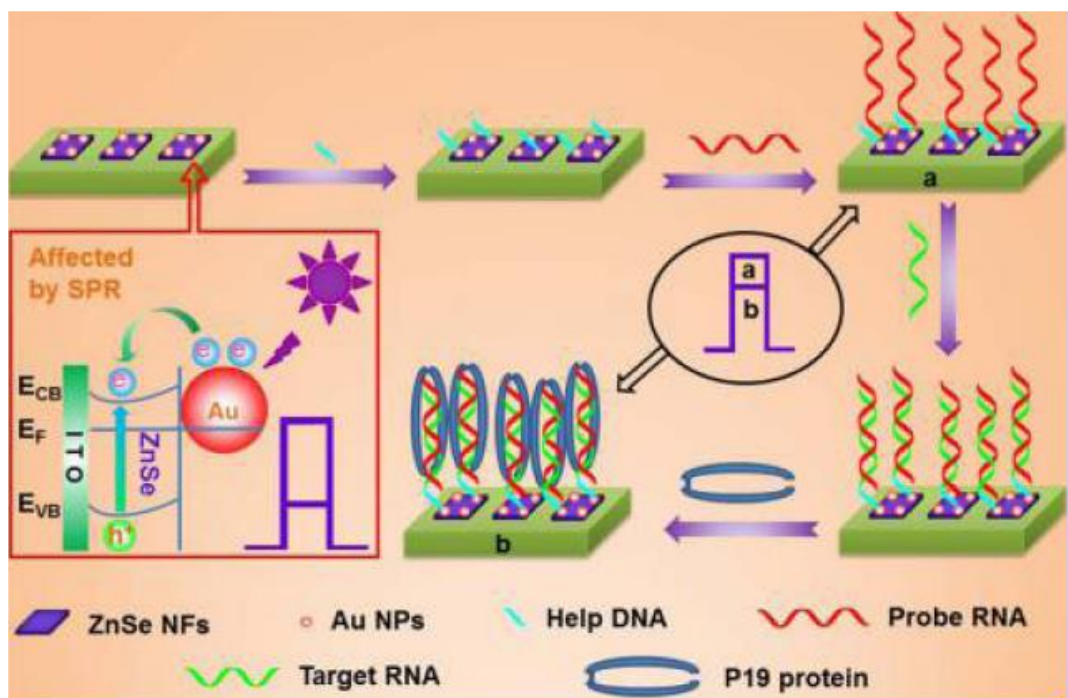


**Figure 10.** Schematic illustration of the PEC biosensing platform based on SPR of Au NPs enhanced RET and remarkable steric hindrance of p19 protein as dual signal amplification. Reprinted with permission from reference [41]. Copyright 2016 American Chemical Society.

P19 protein found in carnation Italian ring spot virus can bind to 21 ~ 23 bp dsRNA with high affinity and sequence independent manner. Based on the dsRNA-p19 interaction, Dai and co-workers reported a PEC biosensor to analyze the level of miRNA-122a in HeLa cells (Figure 10) [41]. In this

work, p19 protein acted as the dsRNA recognition element. The change of PEC signal is dependent upon the target miRNA concentration in a linear range of 350 fM ~ 5 nM with a detection limit of 153 fM. In this strategy, water-soluble ZnSe-COOH nanosheets (NFs) modified with AuNPs were used as the signal reporters. Due to local surface plasmon resonance (LSPR) of AuNPs, the ultraviolet-visible absorption spectra of Au NPs overlapped with the emission spectra of ZnSe-COOH NFs, resulting in effective resonance energy transfer (RET) between ZnSe-COOH NFs and AuNPs. This improved the photoelectric conversion efficiency and amplified the PEC signal. The binding of p19 protein to 21 – 23 bp dsRNA produced a significant steric hindrance, thus limiting the interfacial electron transfer and preventing AA from entering into the holes on the electrode surface. This led to a great decrease in the PEC current intensity.

## 2.6 Immobilization-free

The simplest and most direct PEC DNA detection strategy is to oxidize DNA (especially G residues) directly on semiconductor electrodes as a source of analytical signals. The amount of oxidized DNA reflects the amount of DNA captured or damaged. Therefore, *in situ* label-free detection can be achieved by monitoring the internal reaction of target DNA. This protocol greatly simplifies the sensing scheme. Li's group reported an immobilization-free diffusivity-mediated PEC strategy for miRNA assays using methylene blue (MB) as the photoactive probe and bare ITO glass as the working electrode (Figure 11) [42]. The hybridization between the target miRNAs and the MB-labeled ssDNA probe (MB-DNA) triggered the digestion of MB-DNA by T7 exonuclease (T7 Exo), thus leading to the generation of MB-labeled mononucleotide. The released target miRNAs can initiate the subsequent cycling processes to generate a large amount of MB-labeled mononucleotides. Due to the difference in the diffusivity between MB-DNA and MB-labeled mononucleotide, a significantly enhanced photocurrent signal was observed after the cycling. Therefore, a facile and highly sensitive immobilization-free PEC miRNAs assay was readily realized by the “signal-on” format and the signal amplification of T7 Exo. This method shows a detection limit down to 27 aM. Moreover, this strategy exhibits excellent specificity and can be used to detect miRNAs spiked in serum samples.

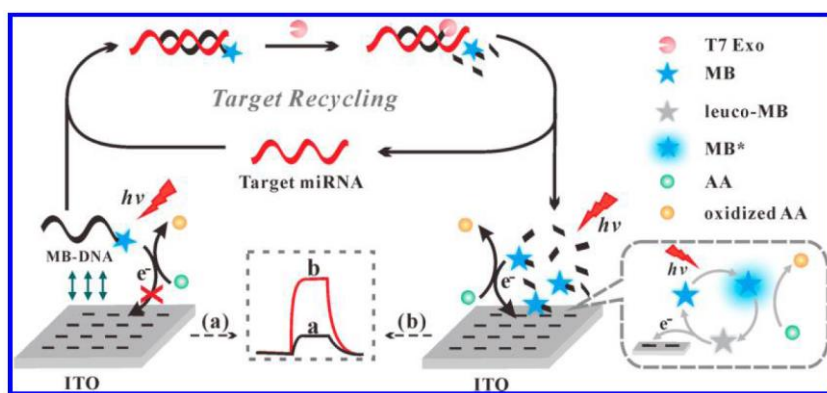


**Figure 11.** Schematic illustration of the immobilization-free diffusivity-mediated PEC strategy for miRNA assay: (a) in the absence and (b) in the presence of the target miRNA. Reprinted with permission from reference [42]. Copyright 2018 American Chemical Society.

### 3. CONCLUSION

PEC biosensors are superior to other micro-analysis methods in view of their low background value, low detection limit and high sensitivity. In addition, the biosensors are simple and easy to operate. So they are widely used in water quality analysis, trace element detection in organisms, food additives and medical assistant analysis. However, the practical applications of PEC are still in the preliminary stage. First, there are fewer kinds of luminescent materials. Second, the preparation technology is not mature and the large-scale production is limited. In addition, the photoelectric conversion efficiency of existing optoelectronic materials needs to be further improved. Therefore, the research, development and applications of new photoelectric materials may become one of the hotspots in this field in the future. At the same time, it will greatly expand the application scope of PEC biosensors. At present, a series of different types of carbon and metal based semiconductor materials have been developed in the field of PEC biosensors. These photoelectric sensing materials and thin films can be directly applied to the rapid PEC detection of electroactive organic or inorganic small molecules/ions. They can also be combined with biomacromolecules including miRNAs or molecular imprinting recognition systems to develop highly sensitive and selective PEC bioanalytical methods. However, the existing optoelectronic materials or thin films still have many shortcomings in the practical application process, such as low conversion efficiency, poor stability, poor uniformity and so on, which greatly limits the further improvement of the performance of the optoelectronic chemical sensors. Among them, metal-based semiconductor materials represented by CdS QDs have been proved to have excellent conversion efficiency and analytical performance, but there are some problems such as strong oxidation ability or toxic heavy metal elements. Therefore, carbon-based semiconductor optoelectronic materials, such as fullerenes, carbon nitride and carbon dots, will receive more attention. On the other hand, at present, a large number of PEC biosensors use dropping coating, immersion and other methods to fabricate semiconductor films, which have relatively poor uniformity and reproducibility, resulting in difficulties in coupling with light sources, limiting their application in space-resolved PEC sensing methods. Therefore, the development of high conversion efficiency, high uniformity, high stability and narrow band gap photoelectric thin films with high efficiency and controllable fabrication scheme and application system will be the key research direction in the field of PEC sensing in the future.

### ACKOWLEDGMENTS

Partial support of this work by the Natural Science Foundation of Henan Province (182300410162) and the Natural Science Foundation of Hunan Province of China (2018JJ3300) was acknowledged.

### References

1. H. Dong, J. Lei, L. Ding, Y. Wen, H. Ju and X. Zhang, *Chem. Rev.*, 113 (2013) 6207.
2. J. Li, S. Tan, R. Kooger, C. Zhang and Y. Zhang, *Chem. Soc. Rev.*, 43 (2014) 506.
3. N. Xia, Y. J. Zhang, X. Wei, Y. P. Huang and L. Liu, *Aanl. Chim. Acta*, 878 (2015) 95.
4. L. Liu, Y. P. Gao, H. P. Liu and N. Xia, *Sensor. Actuat. B: Chem.*, 208 (2015) 137.
5. N. Xia, K. Liu, Y. Zhou, Y. Li and X. Yi, *Int. J. Nanomed.*, 12 (2017) 5013.

6. L. Liu, N. Xia, H. P. Liu, X. J. Kang, X. S. Liu, C. Xue and X. L. He, *Biosens. Bioelectron.*, 53 (2014) 399.
7. F. Li, B. Zhou and W. Zhang, *Int. J. Electrochem. Sci.*, 13 (2018) 7183.
8. C.-D. Chen, M. La and B.-B. Zhou, *Int. J. Electrochem. Sci.*, 9 (2014) 7228.
9. A. A. Jamali, M. Pourhassan-Moghaddam, J. E. N. Dolatabadi and Y. Omidi, *Trac-Trend. Anal. Chem.*, 55 (2014) 24.
10. B. N. Johnson and R. Mutharasan, *Analyst*, 139 (2014) 1576.
11. M. La, L. Liu and B.-B. Zhou, *Materials*, 8 (2015) 2809.
12. N. Xia, B. Zhou, N. Huang, M. Jiang, J. Zhang and L. Liu, *Biosens. Bioelectron.*, 85 (2016) 625.
13. Y. Zang, X. Hu, H. Zhou, Q. Xu, P. Huan and H. Xue, *Int. J. Electrochem. Sci.*, 13 (2018) 7558.
14. X. Cong, M. Zhou, T. Hou, Z. Xu, Y. Yin, X. Wang and M. Yin, *Electroanalysis*, 30 (2018) 1140.
15. Z. Y. Ma, F. Xu, Y. Qin, W. W. Zhao, J. J. Xu and H. Y. Chen, *Anal. Chem.*, 88 (2016) 4183.
16. M. Li, C. Xiong, W. Liang, R. Yuan and Y. Chai, *Anal. Chem.*, 90 (2018) 8211.
17. Y. Zheng, W. Liang, C. Xiong, Y. Zhuo, Y. Hai and R. Yuan, *Anal. Chem.*, 89 (2017) 9445.
18. L. Liu, D. Deng, Y. Wang, K. Song, Z. Shang, Q. Wang, N. Xia and B. Zhang, *Sensor. Actuat. B: Chem.*, 266 (2018) 246.
19. L. Liu, N. Xia, M. Jiang, N. Huang, S. Guo, S. Li and S. Zhang, *J. Electroanal. Chem.*, 754 (2015) 40.
20. L. Liu, Y. Gao, H. Liu, J. Du and N. Xia, *Electrochim. Acta*, 139 (2014) 323.
21. F. Bettazzi, S. Laschi, D. Voccia, C. Gellini, G. Pietrapiezzi, L. Falciola, V. Pifferi, Testolin, A., C. Ingrosso, T. Placido, R. Comparelli, M. L. Curri and I. Palchett, *Electrochim. Acta*, 276 (2018) 389.
22. J. Zhuang, B. Han, W. Liu, J. Zhou, K. Liu, D. Yang and D. Tang, *Biosens. Bioelectron.*, 99 (2018) 230.
23. H. Yin, Y. Zhou, B. C. Li, X. Li, Z. Yang, S. Ai and X. Zhang, *Sensor. Actuat. Chem: B*, 222 (2016) 1119.
24. M. H. Wang, H. S. Yin, Y. L. Zhou, J. R. Han, T. Q. He, L. Cui and S. Y. Ai, *Microchim. Acta* (2018) 185.
25. B. Li, H. Yina, Y. Zhoua, M. Wang, J. Wang and S. Ai, *Sensor. Actuat. Chem: B*, 192 (2017) 0925.
26. H. S. Yin, M. Wang, Y. L. Zhou, X. Y. Zhang, B. Sun, G. H. Wang and S. Y. Ai, *Biosens. Bioelectron.*, 53 (2014) 175.
27. B. Li, X. Li, M. Wang, Z. Yang, H. Yin and S. Ai, *J. Solid State Electrochem.*, 19 (2015) 1301.
28. M. Wang, H. Yin, N. Shen, Z. Xu and B. Sun, *Biosens. Bioelectron.*, 53 (2014) 232.
29. S. Yu, Y. Wang, L. P. Jiang, S. Bi and J. J. Zhu, *Anal. Chem.*, 90 (2018) 4544.
30. B. Wang , Y. X. Dong, Y. L. Wang , J. T. Cao, S. H. Ma and Y. M. Liu, *Sensor. Actuat. Chem: B*, 254 (2018) 159.
31. Y.-X. Dong, J.-T. Cao, B. Wang, S.-H. Ma and Y.-M. Liu, *ACS Sustainable Chem. Eng.*, 5 (2017) 10840.
32. A. A. Tahir, M. A. Ehsan, M. Mazhar, K. G. U. Wijayantha, M. Zeller and A. D. Hunter, *Chem. Mater.*, 22 (2010) 5084.
33. S. Wang, X. Li, Y. Chen, X. Cai, H. Yao, W. Gao, Y. Zheng, X. An, J. Shi and H. Chen, *Adv. Mater.*, 27 (2015) 2775.
34. C. Ye, M. Q. Wang, Z. F. Gao, Y. Zhang, J. L. Lei, H. Luo, Q, and N. B. Li, *Anal. Chem.*, 88 (2016) 11444.
35. Y. Wang, H. Shi, K. Cui, L. Zhangb, S. Gec, M. Yan and J. Yu, *Biosens. Bioelectron.*, 117 (2018) 515.
36. X. Pang, J. Qi, Y. Zhang, Y. Ren, M. Su, Jia, B., Y. Wang, Q. Wei and B. Du, *Biosens. Bioelectron.*, 85 (2016) 142.
37. C. Ye, M. Q. Wang, H. Q. Luo and N. B. Li, *Anal. Chem.*, 89 (2017) 11697.

38. Y. N. Zheng, W. B. Liang, C. Y. Xiong, Y. L. Yuan, Y. Q. Chai and R. Yuan, *Anal. Chem.*, 88 (2016) 8698.
39. M. Wang, Z. Yang, Y. Guo, X. Wang, H. Yin and S. Ai, *Microchim. Acta*, 182 (2015) 241.
40. N. Fu, Y. S. Hu, S. Shi, W. Ren, S. Liu, B. Su, L. Zhao, W. L. and L. Wang, *Analyst*, (2018) 1.
41. W. Tu, H. Cao, L. Zhang, J. Bao, X. Liu and Z. Dai, *Anal. Chem.*, 88 (2016) 10459.
42. T. Hou, N. Xu, W. Wang, L. Ge and F. Li, *Anal. Chem.*, 90 (2018) 9591.

© 2019 The Authors. Published by ESG ([www.electrochemsci.org](http://www.electrochemsci.org)). This article is an open access article distributed under the terms and conditions of the Creative Commons Attribution license (<http://creativecommons.org/licenses/by/4.0/>).